A 200 GHz Fully Integrated Quasi-Optical Detector Using Orthogonal Heterostructure Backward Diodes with Improved Performance

Yu Shi[1*], Yijing Deng[1], Peizhao Li[1], Patrick Fay[1], and Lei Liu[1]

Abstract— **In this paper, we report the updated results of a 200 GHz fully integrated quasi-optical detector based on orthogonal heterostructure backward diodes. The newly fabricated devices and detector circuit have been characterized through on-wafer dc and RF tests. An improved voltage responsivity as high as 500 V/W has been projected for the integrated detector.**

Keywords— **Backward diode, on-wafer measurement, terahertz detector.**

I. Introduction

Terahertz (THz) detector has drawn increasing attentions for potential applications in radio astronomy, biomedical imaging, and remote detection. Most detectors can only sense the amplitude or the phase of the THz wave. However, the polarization of the THz wave can also provide important information about the object under test, which accelerates the development of highly sensitive polarization resolved THz detector.

In our previous paper [1], a fully integrated dual polarization quasi-optical detector based on zero-bias heterostructure backward diodes (HBDs) was proposed and a reduced voltage responsivity was reported. The polarization imaging capability of such device has also been demonstrated [2]. In order to analyze the results and improve the detector performance, additional on-wafer test structures have been fabricated and characterized. An improved voltage responsivity as high as 500 V/W can be projected for the newly developed detector based on the on-wafer measurement results.

II. Device Characterization

The design and fabrication of the proposed detector has been described in [1]. In order to evaluate the performance of the detector, additional HBDs with a ground-signal-ground (GSG) probe pad have been fabricated along with the integrated detector and then characterized.

The devices were tested first through on-wafer dc measurement (see Fig. 1(a)), from which the IV curve can be obtained. The IV curve of the 1.5 µm × 1.5 µm HBD, as well as the corresponding curvature coefficient, are shown in Fig. 1(b). It can be seen that a curvature coefficient of -27 V^{-1} has been achieved for the HBD at zero bias. The curvature coefficient is higher than the results reported in [1], leading to an improved voltage responsivity.

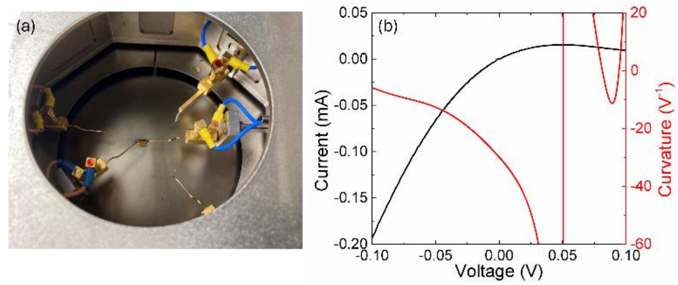

Fig. 1. (a) on-wafer dc measurement setup; (b) IV curve and the corresponding curvature coefficient of the 1.5 µm × 1.5 µm HBD.

For the small signal on-wafer RF measurements at 200 GHz, the same HBD with a GSG probe pad was characterized. The experiment setup is shown in Fig. 2(a). An Agilent E8361C vector network analyzer (VNA) with WR-5.1 band extenders (from OML Inc.) was used. An additional piece of AlN absorber was placed in between the chip and the chuck of the probe station to minimize the reflection.

In order to transfer the reference plane to the tip of the GSG probe, on-wafer calibration was first performed with the off-chip Line-Reflect-Reflect-Match (LRRM) standards. Additional on-chip Through-Reflect-Line (TRL) standards, which were fabricated along with the devices, were used to de-embed the GSG probe pad so that the intrinsic S-parameters of the HBD can be obtained. The intrinsic S_{11} from 140 GHz to 220 GHz is shown in Fig. 2(b).

The lumped element model of the device after de-embedding is shown in Fig. 3(a). In addition to the junction resistor (R_j), junction capacitor (C_j), and series resistor (R_s) from the intrinsic HBD, the model also includes a parasitic inductor L_p from the metal airbridge and the warped ground, and a parasitic capacitor C_p from the metal contacts. Their values can be obtained from

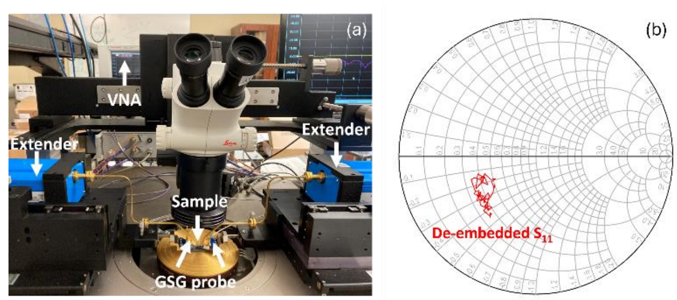

Fig. 2. (a) The experiment setup of the on-wafer small signal S parameter measurement; (b) The intrinsic S_{11} of the 1.5 µm × 1.5 µm HBD.

[1]Department of Electrical Engineering, University of Notre Dame, Notre Dame IN, 46556. [*]Corresponding author (email: yshi5@nd.edu).

NOTES:

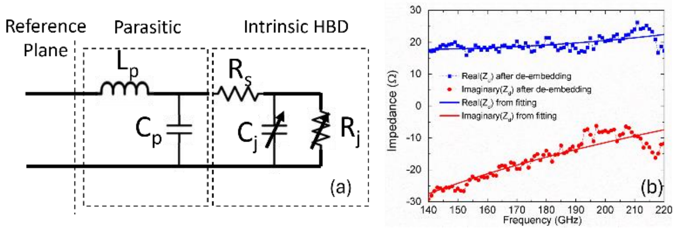

Fig. 3. (a) The lumped element model of the device; (b) The real and the imaginary part of the device impedance (Z_d) from measurement (dotted line) and from fitting (solid line).

TABLE 1. HBD Key Parameter Comparison

	This work	Ref [3]	Ref [4]	Ref [5]
Curvature (V^{-1})	-27	-47	-25	-39
Area (μm²)	1.5 × 1.5	0.4 × 0.4	1 × 1	2 × 2
Barrier thickness (nm)	1.47	1.1	1	3.2
R_j (Ω· μm²)	14.6×10^3	814	1045	55.6×10^3
C_j (fF/ μm²)	11.3	15	8.5	7.2
R_s (Ω· cm²)	4.3×10^{-7}	2.0×10^{-7}	2.2×10^{-7}	2.2×10^{-7}
Cut-off frequency (GHz)	328	644	850	740

fitting the device impedance (Z_d) after de-embedding. The impedance from the lumped element model, as well as that from the measurement after de-embedding, are shown in Fig. 3(b). It can be seen that the results matched well with each other, showing the effectiveness of the lumped element model and the fitting process.

The extracted key device parameters of the HBD, as well as those from the previous work [3][4][5] are summarized in Table 1. It can be seen that the R_j increased with the thickness of the barrier, as expected. The R_s also became larger than the previous results, leading to a degraded cut-off frequency. The additional parasitic elements also lead to power reflection and decrease the detector responsivity since the matching condition is not satisfied.

III. CIRCUIT CHARACTERIZATION

In addition to the HBD, the annular slot antenna, as well as the orthogonal detector circuit, were also characterized through the same on-wafer S-parameter measurement. In order to obtain the intrinsic S-parameters, the same de-embedding process as mentioned earlier has been performed.

The S_{11} of the antenna after de-embedding are shown in Fig. 4(a). The S_{11} from the full wave simulation are also plotted for comparison. It can be seen that the measurement results have an offset of around 5 GHz (2.5%) compared with the simulation, which is due to the feeding signal line that was left after de-embedding the GSG probe pad.

The S-parameters of the entire detector circuit including the shorted stubs, the interdigitated dc block, and the low pass filter were also obtained. Both the measurement and the simulation results are shown in Fig. 4(b). It can be seen that the on-wafer

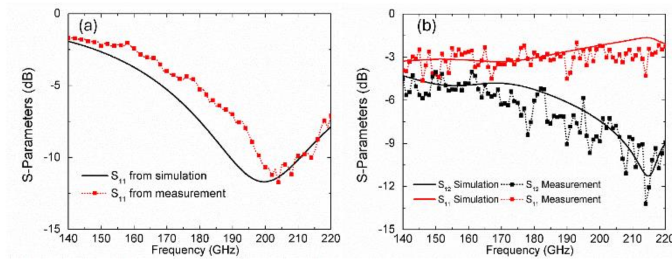

Fig. 4. (a) Measured (solid) and simulated (dotted) S_{11} of the annular slot antenna; (b) Measured (solid) and simulated (dotted) S_{11} and S_{12} of the detector circuit in one polarization.

measurement results are close to the simulation, with discrepancy likely from the noise during the measurement.

On the basis of the on-wafer dc and RF measurement results, the circuit model of the entire detector was extracted. The detector voltage responsivity can therefore be projected to be as high as 500 V/W, much higher than the results reported in [1]. This improvement in responsivity can also benefit the polarization imaging capability of the proposed integrated detector since the angular resolution of the imaging system can increase [2]. The performance could be further improved by reducing the insertion loss of the detector circuit, as well as eliminating the impedance mismatch that came from the parasitic elements.

IV. CONCLUSION

In this paper, the measurement results of the HBDs and detector circuits through on-wafer dc and RF tests were presented. An improved responsivity of the integrated detector can therefore be projected. The results show the promises of the integrated detector for THz polarization detection in remote sensing, biomedical imaging, and radio astronomy.

REFERENCES

[1] Y. Shi, Y. Deng, P. Li, P. Fay and L. Liu, "*A 200 GHz Fully Integrated, Polarization-Resolved Quasi-Optical Detector Using Zero-Bias Heterostructure Backward Diodes*," IEEE Microwave and Wireless Components Letters, vol. 32, no. 7, pp. 891-894, July 2022.

[2] Y. Shi, Y. Deng, P. Li, P. Fay and L. Liu, "*Polarization-Resolved THz Imaging with Orthogonal Heterostructure Backward Diode Detectors,*" in IEEE Transactions on Terahertz Science and Technology, vol. 13, no. 3, pp. 286-296, May 2023.

[3] Z. Zhang, R. Rajavel, P. Deelman, and P. Fay, "*Sub-Micron Area Heterojunction Backward Diode Millimeter-Wave Detectors with 0.18 pW/Hz1/2 Noise Equivalent Power*," IEEE Microw. Wireless Components Lett., vol. 21, no. 5, pp. 267-269, 2011.

[4] Z. Zhang, "*Sb-heterojunction backward diodes for direct detection and passive millimeter-wave imaging*," Ph.D. dissertation, Dept. Elect. Eng., Univ. Notre Dame, Notre Dame, IN, USA, 2011

[5] N. Su, R. Rajavel, P. Deelman, J. N. Schulman and P. Fay, "*Sb-Heterostructure Millimeter-Wave Detectors With Reduced Capacitance and Noise Equivalent Power*," in IEEE Electron Device Letters, vol. 29, no. 6, pp. 536-539, June 2008

NOTES: